Journal of Medicinal Chemistry

Article

pubs.acs.org/jmc

Identification of a Promising Drug Candidate for the Treatment of Type 2 Diabetes Based on a $P2Y_1$ Receptor Agonist[¶]

Shir Yelovitch,[†,∥] Haim M. Barr,[‡,∥] Jean Camden,[§] Gary A. Weisman,[§] Ela Shai,[⊥] David Varon,[⊥] and Bilha Fischer*[,†]

[†]Department of Chemistry, Bar-Ilan University, Ramat-Gan 52900, Israel

[‡]BioLineRx Ltd., 23 Hillel Street, Jerusalem 91450, Israel

[§]Biochemistry Department, 540E Bond Life Sciences Center, University of Missouri, Columbia, Missouri 65211, United States

[⊥]Department of Hematology, Hadassah University Hospital, Jerusalem 91120, Israel

ABSTRACT: The activation by extracellular nucleotides of pancreatic P2Y receptors, particularly, the $P2Y_1R$ subtype, increases insulin secretion. Therefore, we developed analogues of the $P2Y_1R$ receptor agonist 2-MeS-ADP, as potential antidiabetic drugs. Analogue **3A** was found to be a potent $P2Y_1R$ agonist (EC_{50} = 0.038 μM vs 0.0025 μM for 2-MeS-ADP) showing no activity at $P2Y_{2/4/6}Rs$. Analogue **3A** was stable at pH 1.4 ($t_{1/2}$ = 7.3 h) and resistant to hydrolysis vs 2-MeS-ADP by alkaline phosphatase ($t_{1/2}$ = 6 vs 4.5 h), human e-NPP1 (4% vs 16% hydrolysis after 20 min), and human blood serum (30% vs 50% hydrolysis after 24 h). Intravenous administration of **3A** in naïve rats decreased blood glucose from 155 mg/dL to normal values, ca. 87 mg/dL, unlike glibenclamide, leading to subnormal values (i.e., 63 mg/dL). Similar observations were made for streptozotocin (STZ)-treated and db^+/db^- mouse models. Furthermore, **3A** inhibits platelet aggregation *in vitro* and elongates bleeding time in mice (iv administration of 30 mg of **3A**/kg), increasing bleeding time to 16 vs 9 min for Prasugrel. Oral administration of 30 mg/kg **3A** to rats increased tail bleeding volume, similar to aspirin. These findings suggest that **3A** may be an effective treatment for type 2 diabetes by reducing both blood glucose levels and platelet aggregation.

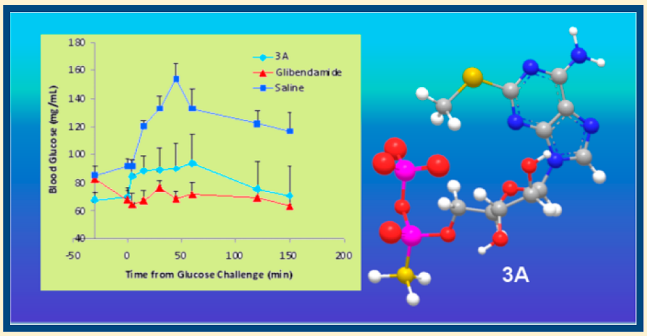

INTRODUCTION

Diabetes mellitus is a chronic, incurable metabolic disorder defined by a dysregulation of glucose homeostasis manifesting as hyperglycemia, abnormalities in lipid and protein metabolism, and the development of both acute and long-term complications.[1,2] Type 2 diabetes is the most prevalent form of the disease, affecting approximately 95% of patients with diabetes. It is characterized by insulin resistance,[3] relatively reduced insulin secretion,[4] or both and is largely the result of excess body weight and physical inactivity.

According to the World Health Organization, type 2 diabetes affects over 170 million people worldwide. This number is expected to double by 2025. Effective glycemic control can lower the incidence of diabetic complications and reduce their severity. Thus, enhancement of insulin secretion in type 2 diabetes is a major therapeutic goal.

Approximately half of the patients with type 2 diabetes are treated with various oral agents that stimulate insulin secretion.[5,6] Among insulin secretagogues, sulfonylureas are the major oral antidiabetic agents currently available. Sulfonylureas elicit insulin secretion by binding to K_{ATP} channels of pancreatic β-cells and inducing their closure.[7] Since this effect of sulfonylureas is not glucose-dependent, the primary side effect is hypoglycemia[8] due to stimulation of insulin secretion at low glucose concentrations. In addition, sulfonylureas have possible long-term adverse effects on the functions of pancreatic β-cells and the cardiovascular system.[9]

Adenine nucleotides (e.g., ATP and ADP) enhance glucose-induced insulin secretion by activating G protein-coupled P2Y receptors in pancreatic β-cells,[10,11] which has been shown to increase the insulin response *in vivo*.[12] A variety of P2 receptor agonists have been shown to stimulate glucose-dependent insulin release in human pancreatic islets.[13] Thus, P2Y receptor agonists show promise in the treatment of type 2 diabetes. ADP and its analogues induce glucose-dependent insulin secretion more potently than ATP and its analogues,[14,15] suggesting a role for an ADP-preferring receptor, such as the $P2Y_1R$.

A role for $P2Y_1R$ activation has been implicated in the maintenance of glucose homeostasis and insulin secretion in mice.[16] Thus, the use of $P2Y_1R$-selective ligands may represent a novel and effective approach for regulating glucose homeostasis in type 2 diabetes. Indeed, we found that α-borano-2-MeS-ATP, analogue **1**, R_p-isomer (Figure 1), is a potent and selective agonist of the $P2Y_1R$ (EC_{50} = 2.6 nM vs 0.2 μM for ATP) in HEK 293 cells overexpressing the $P2Y_1R$.[17]

Received: May 8, 2012
Published: August 8, 2012

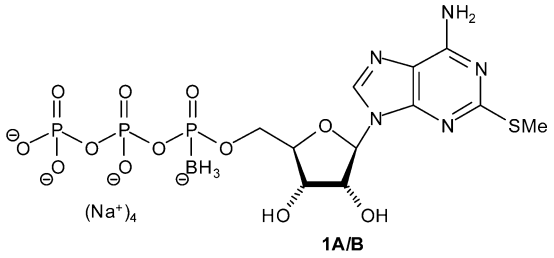

Figure 1. Nucleotide-based insulin secretagogue.

Furthermore, analogue **1A** was shown to be a very potent glucose-dependent insulin secretagogue in isolated rat pancreas at elevated blood glucose levels[15] and thus may minimize the risk of hypoglycemia seen with sulfonylureas. Analogue **1A** increases insulin secretion up to 9-fold greater than basal secretion with an EC_{50} of 28.1 nM.[15] Moreover, analogue **1A** exhibited high stability at physiological and gastric pH at 37 °C, with half-lives of 1395 and 5.9 h, respectively. Yet, analogue **1A** was hydrolyzed almost completely by alkaline phosphatase over 100 min at 37 °C.[18]

In this study, we attempted to develop an insulin secretagogue based on the structure of $P2Y_1R$ agonists (i.e., ADP and 2-MeS-ADP) that is metabolically stable under physiological conditions. Since the most potent $P2Y_1R$ agonists are ADP and its analogues, we chose to use the ADP(α-B) scaffold to synthesize potential drug candidates. The ADP(α-B) scaffold is expected to be resistant to enzymatic hydrolysis by alkaline phosphatase, eNPP1 (ecto-nucleotide pyrophosphatase, EC 3.1.4.1), or NTPDase (ecto-nucleoside triphosphate diphosphohydrolase, EC 3.6.1.5) because of the proximity of the borane moiety to the cleavage site of ADP between Pα and Pβ. In addition, we synthesized analogues that incorporate a diadenosine polyphosphate scaffold, which has been shown to generate P2 receptor ligands with high enzymatic stability and receptor specificity.[19] In an attempt to enhance agonist potency and selectivity for the $P2Y_1R$, as previously described,[20,21] we incorporated methylthio groups at the adenine C2 positions of the analogues. Here, we describe the synthesis and characterization of analogues **2**–**4** (Figure 2), and their activities at the $P2Y_1R$ vs the $P2Y_{2/4/6}Rs$. In addition, we report on the chemical stability of the analogues and their resistance to hydrolysis by alkaline phosphatase, human eNPP1, and enzymes in human blood serum. Furthermore, we demonstrate that analogue **3** is an effective modulator of blood glucose and insulin levels *in vivo* in both normal and diabetic mice and rats and also acts as an inhibitor of platelet aggregation.

RESULTS

Synthesis of Analogues 2 and 3. Since 2-MeS-ADP is among the most potent $P2Y_1R$ agonists currently known, we chose 2-MeS-adenosine as the starting material for the preparation of 2-MeS-ADP-α-B, analogue **3**. We synthesized 2-MeS-ADP(α-B), analogue **3** in a one-pot, five-step synthesis outlined in Scheme 1. In addition, to determine whether a 2-MeS substitution enhances agonist activity and enzymatic stability in comparison to ADP-α-B, analogue **2**, the latter was also synthesized as described in Scheme 1.[22] The use of phosphitylation and boranation reagents in the synthetic method depicted in Scheme 1 requires protected nucleosides. It has been shown that protection of the adenine N^6-position is not required, but selectivity for the 5′-OH in the initial phosphitylation step is marginal if the 2′- and 3′-OH are not protected.[23] To minimize the number of synthetic steps, we chose a methoxymethylidene protecting group that is selective for 2′,3′-hydroxyl groups, thus avoiding protection of the 5′-OH, and this protecting group remained throughout the entire synthesis. In the last step of the boranation reaction in Scheme 1, the protecting group was removed under mild conditions that do not affect the formed boranophosphate moiety or the N-glycosidic bond. Removal of the methoxymethylidene group involved a hydrolysis step at pH 2.3 and another at pH 9,[24,25] at which point product **11** was stable. Furthermore, both of these steps were relatively rapid, lasting less than 4 h, compared with 24–48 h required for the removal of alternative acetate protecting groups. Methoxymethylidene-protected nucleoside **5** (Scheme 1) was treated with 2-chloro-4*H*-1,3,2-benzodioxaphosphorine-4-one in dry dioxane to form the activated phosphate intermediate **6**, to which bis(tributylammonium) pyrophosphate salt was added at room temperature yielding the cyclic triphosphate intermediate **7**, which underwent a subsequent boranation step to yield product **8**. A slight excess of 2-chloro-4*H*-1,3,2-benzodioxaphosphorine-4-one (1.1 equiv) and pyrophosphate tributylammonium salt (1.5 equiv) was used to ensure the complete formation of intermediate **6** and possibly intermediate **7**. Among borane complexes that react as Lewis acids, we selected borane-dimethylsulfide, a boranation reagent that is effective under mild conditions (i.e., for 15 min at room temperature). Coordination of the electron-deficient borane of borane-dimethylsulfide with cyclic trivalentphosphorous intermediate **7**, a Lewis base, yielded intermediate **8**. In the same pot, intermediate **8** was reacted with ethylenediamine at room temperature to form methoxymethylidine-protected 2-MeS-ADP(α-B) analogue **11**. After purification of analogue **11** on an anion exchange column, the methoxymethylidene protective group was removed, as described above, to generate analogue **3** at a 40% yield after LC separation.

The identity and purity of analogue **3** were established by ^1H and ^{31}P NMR, ESI, and MALDI negative mass spectrometry and HPLC using two solvent systems. ^{31}P NMR spectra of analogue **3** showed a typical Pα signal as a multiplet at about 84 ppm. ^1H NMR spectra showed borane hydrogen atoms as a very broad signal at about 0.3 ppm. Due to the chiral center at

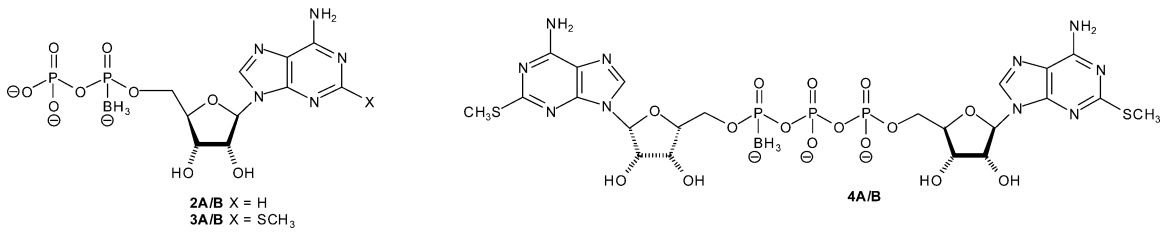

Figure 2. ADP(α-B) analogues tested as $P2Y_1R$ agonists.

dx.doi.org/10.1021/jm3006355 | J. Med. Chem. 2012, 55, 7623–7635

Scheme 1. One-Pot Synthesis of 2-MeS-Adenosine 5′-*O*-(α-Borano)diphosphate, Analogue 3A[a]

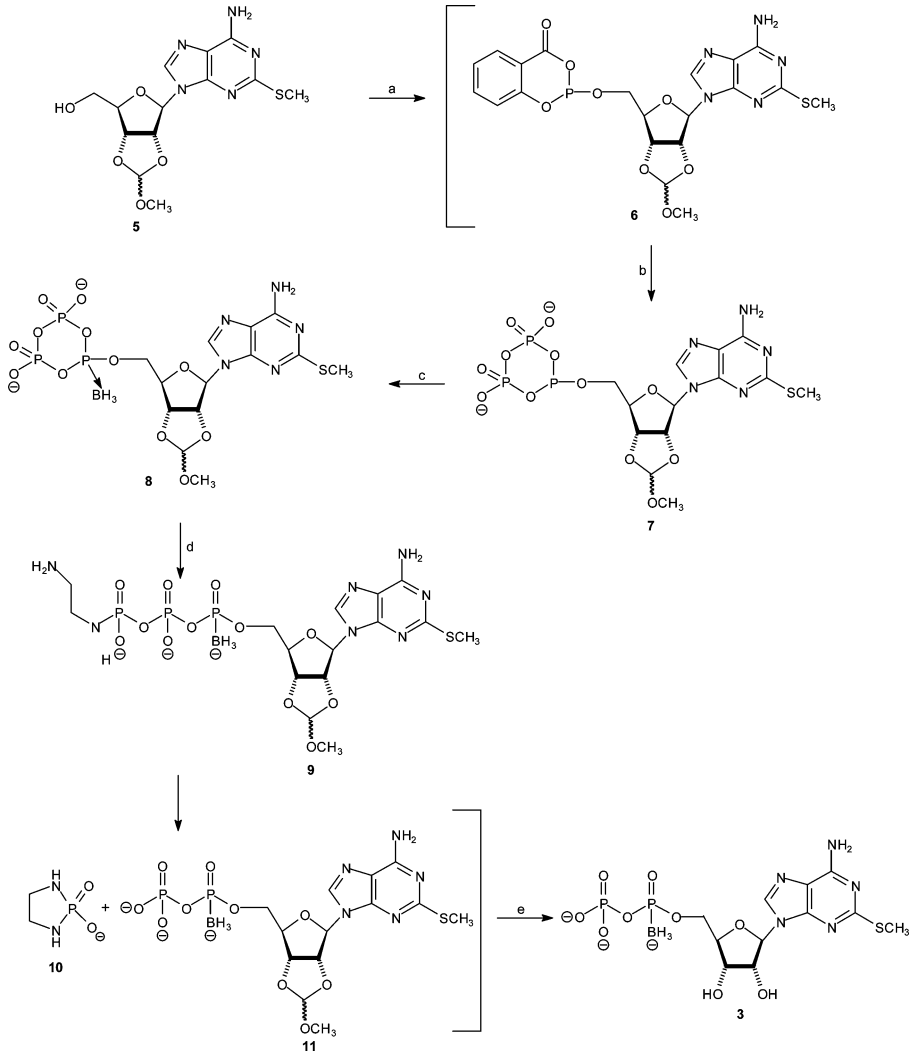

[a]Reaction conditions: (a) DMF/pyridine/dioxane, salicylphosphochloridite, RT, 10 min; (b) $P_2O_7H_2^{2-}(Bu_3NH^+)_2$/DMF, Bu_3N, RT, 10 min; (c) 2 M BH_3/SMe_2 in THF, RT, 15 min; (d) (1) $NH_2CH_2CH_2NH_2$, RT, 1 h; (2) dist H_2O, RT, 30 min; (e) (1) pH 2.3, RT, 3 h; (2) pH 9, RT, 45 min.

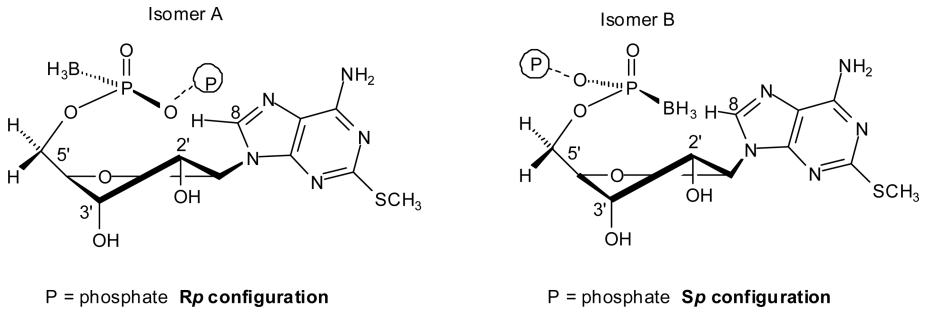

Figure 3. Conformation of P-diastereomers of analogue **3**.

Pα, analogue **3** was obtained as a pair of diastereoisomers in a 1:1 ratio. In both ^1H and ^{31}P NMR spectra, there are slight differences between the chemical shifts for the two diastereoisomers.

Determination of the Absolute Configuration of Analogue 3 Diastereoisomers. Analogue **3** diastereomers were efficiently separated by reverse-phase HPLC using 100 mM triethylammonium acetate (pH 7)/acetonitrile, with a 1−2 min difference in their retention times. The separated diastereomers were designated as diastereomer A and diastereomer B with the A isomer eluting before the B isomer.

The spectral characteristics of analogue **3A** and **3B** isomers were very similar except for changes in the chemical shifts of H8 and Pα in ^1H and ^{31}P NMR spectra (H8 at 8.45 and 8.42 ppm and Pα at 83.0 and 84.1 ppm for **3A** and **3B** isomers, respectively). Prior assignment of configurations for NDPαS and NDPαSe were S_p and R_p for these first and second eluting diastereomers, respectively.[26] Since the group priorities around

dx.doi.org/10.1021/jm3006355 | J. Med. Chem. 2012, 55, 7623−7635

Pα for NDPαS and NDPαSe are opposite to those of NDPαB (Figure 3) and assuming that the same order of elution occurs with analogues **3A** and **3B** (NDPαB) compared with NDPαS and NDPαSe, the assignment of configuration for NDPαB is R_p and S_p for analogues **3A** and **3B**, respectively. This assignment of the absolute configuration for ADPαB is consistent with the opposite stereospecificity toward S_p and R_p selective enzymes.[27] The assignment of the absolute configuration for both diastereomers is further confirmed by ^{1}H NMR. A difference in the chemical shift of H8 is observed between the two diastereoisomers, as shown in Table 1. The signal of H8 of the

Table 1. Chemical Shifts of Analogue 3 Isomers in D_2O

	H5″	H5′	H4′	H3′	H2′	H1′	H8
3A R_p-isomer	4.00	4.12	4.24	4.47	4.60	5.99	8.45
3B S_p-isomer	4.00	4.12	4.25	4.39	4.62	5.99	8.42

B isomer of analogue **3** in ^{1}H NMR spectra is more shielded than the signal of H8 of the A isomer due to the influence of the vicinal BH_3 group on Pα (8.45 vs 8.42 ppm). This small, although indicative, Δδ between H8 of A and B isomers may be explained in terms of the closer proximity to H8 of the negative charge on BH_3 compared with O for the B isomer (Figure 3) and is due to the longer P−B bond (1.89 Å) compared with P−O (1.60 Å), in addition to the contribution of the B−H bond (1.25 Å).[28] Furthermore, the upfield shift of H8 of the B isomer may be due to an unconventional H-bond between the BH_3 group and the relatively acidic H8[29] that is known to exist between borane-amines and acidic protons.[30] Such a preferential intramolecular H-bond results in the shielding of H8. Previous calculations[25] indicate that Pα is much further away from H8 in the A isomer than in the B isomer. Thus, the S_p configuration can be attributed to analogue **3B** and R_p to analogue **3A** of 2-MeS-ADP(α-B).

Synthesis of Analogue 4. Dinucleoside polyphosphates are conventionally prepared via the activation of the 5′ terminal phosphates of a nucleotide with carbonyl diimidazole (CDI),[31] thereby forming a phosphoryl donor (P-donor) that reacts with a nonactivated nucleotide (i.e., phosphoryl acceptor (P-acceptor)). We attempted two different approaches to synthesize analogue **4**. In the first approach, analogue **12** was activated with CDI to generate the P-donor and analogue **13** was the P-acceptor (Scheme 2). In the second approach, CDI-activated analogue **13** was the P-donor and analogue **12** was the P-acceptor. The activation of analogues **12** and **13** with CDI was monitored by TLC, which showed that analogue **12** reacted completely with CDI after 3 h, whereas the activation of analogue **13** was incomplete over this time period, likely due to the low nucleophilicity of the phosphate group in analogue **13**. Therefore, we chose to synthesize analogue **4** by activating analogue **12** with CDI.

Briefly, the synthesis of analogue **4** involved the activation of the 2-MeS-AMP$(Bu_3NH)_2^+$ salt with CDI in dry DMF at room temperature for 3 h, followed by the addition of the bis$(Bu_4N)^+$ salt of 2-MeS-ADP(α-B) and $MgCl_2$. After 12 h at room temperature, analogue **4** was formed as the exclusive product at 80% yield after LC separation. Due to the chiral center at Pα, analogue **4** was obtained as a pair of diastereoisomers in a 1:1 ratio. Each diastereoisomer exhibits a characteristic ^{31}P NMR spectrum showing three signals: 87 (m, Pα-B), −10.5 (d, Pα), and −21.5 (dd, Pβ) ppm.

Activity of Analogues 2−4 at the $P2Y_{1/2/4/6}$ Receptors. The activities of analogues **2**−**4** were evaluated at the turkey $P2Y_1$ receptor expressed in human 1321N1 astrocytoma cells that are devoid of endogenous P2Y receptors.[32] The order of potency of agonists for activation of the turkey $P2Y_1$-R was found to be identical to that observed for the human $P2Y_1$-R.[33] $P2Y_1$R activity was determined by monitoring increases in the intracellular calcium concentration, $[Ca^{2+}]_i$, induced by the analogues (Figure 4).

ADP(α-B), analogue **2**, activated the $P2Y_1$R with EC_{50} values of 0.22 and 0.96 μM for isomers **2A** and **2B**, respectively. 2-MeS-ADP(α-B), isomers **3A** and **3B**, exhibited EC_{50} values of 0.038 and 1.1 μM, respectively. Thus, substitution at C2 of ADP(α-B) by an electron-donating 2-MeS group increased by 6-fold the agonist potency of the **3A** isomer at the $P2Y_1$R. 2-MeS-Ap_3(α-B)-A-2-MeS, isomers **4A** and **4B**, had EC_{50} values of 0.14 and 0.19 μM at the $P2Y_1$R, respectively. Here, the contribution of the 2-MeS substitution to ligand activity can be demonstrated by comparing the EC_{50} values of the analogue **4** isomers to those of Ap_3(α-B)A isomers, which are 0.76 and 0.8 μM, respectively.[34] In this case, the MeS substitution at C2 resulted in a 4−6-fold increase in potency, as well. All tested analogues are less potent agonists of the $P2Y_1$R than 2-MeS-ADP (EC_{50} = 0.0025 μM). Thus, the borane group reduces $P2Y_1$R activity by at least 15-fold. The activities of the diastereomers of analogue **4** at the $P2Y_1$R are only slightly

Scheme 2. Synthesis of 2-MeS-AP_3(α-B)-A-2-MeS, Analogue 4[a]

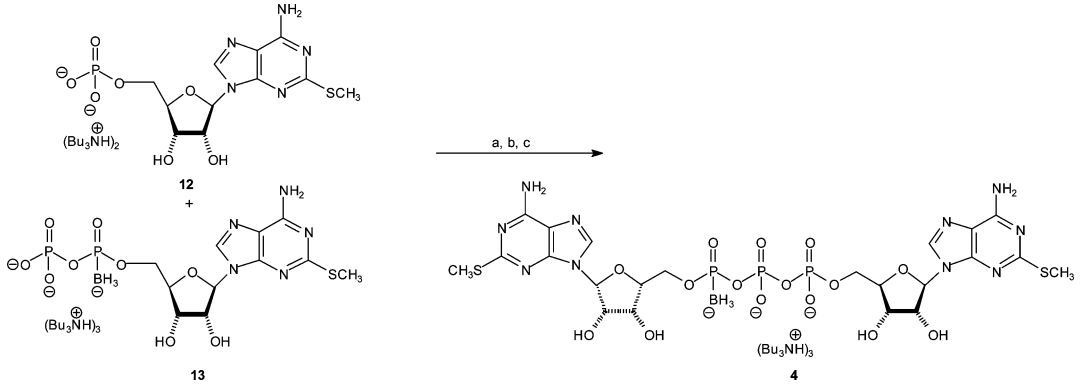

[a]Reaction conditions: (a) CDI (5 equiv), DMF, RT, 3 h; (b) dry MeOH (5 equiv), RT, 8 min; (c) BPi (1 equiv), DMF, $MgCl_2$ (8 equiv), RT, overnight.

dx.doi.org/10.1021/jm3006355 | J. Med. Chem. 2012, 55, 7623−7635

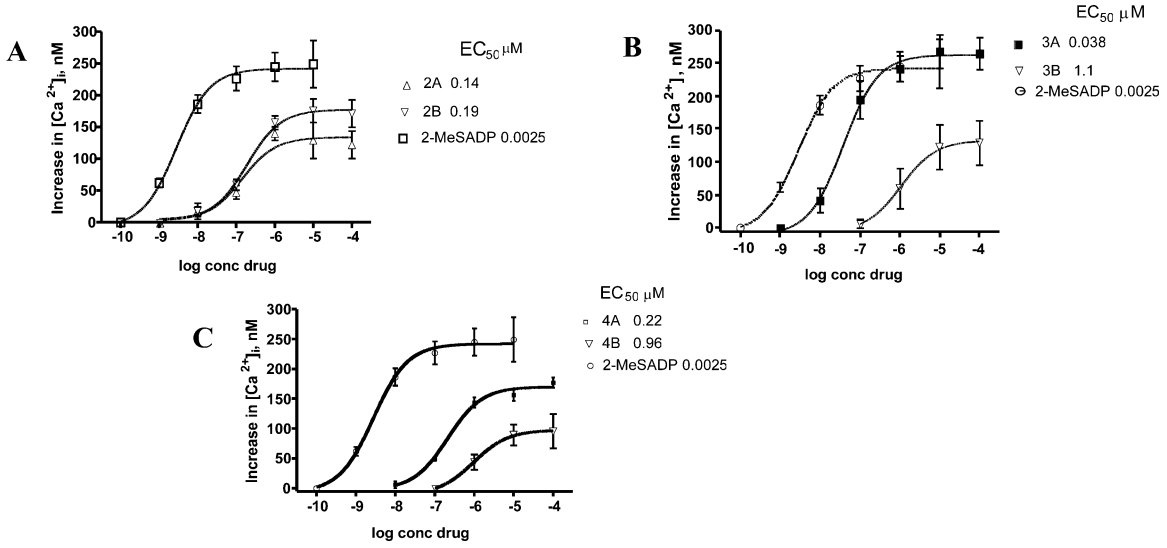

Figure 4. Concentration−response curves for analogues **2**−**4** determined by measuring analogue-induced increases in $[Ca^{2+}]_i$ in human 1321N1 astrocytoma cells stably transfected with the turkey $P2Y_1R$.

different. For the NDP(α-B) analogues **2** and **3**, it was found that the A isomers are ∼4−30-fold more potent in increasing $[Ca^{2+}]_i$ than the corresponding B isomers. Apparently, the A isomers, R_p configuration (Figure 3), promote tighter receptor binding. These analogues were virtually ineffective agonists of the $P2Y_2$, $P2Y_4$, and $P2Y_6$ receptors (data not shown).

Resistance of Analogues 2−4 to Degradation by Alkaline Phosphatase. Alkaline phosphatase (AP) is a hydrolase that catalyzes the removal of a phosphate group from nucleotides to generate inorganic phosphate (Pi) and the corresponding alcohol. AP catalyzes the stepwise production of Pi by ATP hydrolysis to ADP and subsequently AMP.[35] In humans, AP is present in all tissues.[36]

The hydrolysis rates of analogues **2**−**4** by AP were determined by measuring the change in the integrated HPLC peaks for each analogue over time. Results are given for the incubation of 0.5 mg of substrate in 32.5 μL of Tris buffer containing 6.25 units of AP at 37 °C for 8 h. Samples were taken every 1 h. The enzyme was then deactivated by heating to 75 °C for 5 min. As a control, we used a sample that did not contain enzyme to ensure that the tested compounds were not degraded at 75 °C. The half-life of ADP, the endogenous ligand of the $P2Y_1R$, is 4 h under the above conditions, whereas the half-lives of ADP(α-B), **2A**, 2-MeS-ADP, and 2-MeS-ADP(α-B), **3A**, are 4.2, 4.5, and 6 h, respectively (Table 2). 2-MeS-Ap_3(α-B)-A-2-MeS (analogue **4**) is completely resistant to hydrolysis by AP over this time course (Table 2), suggesting that it is not a substrate of the enzyme.

Resistance of Analogues 2−4 to Degradation by Human eNPP1. eNPP1 cleaves NDP into NMP and Pi and Np_nN into NMP and Np_{n-1}. Because members of the eNPP family share an alkaline pH optimum, eNPP1 activity was measured at pH 8.5. Human eNPP1 (11 mg/mL) was added to incubation buffer at 37 °C and preincubated for 3 min, and the reaction was started by addition of 0.2 mM analogue **2**, **3**, or **4** and terminated after 20 min by addition of perchloric acid.[37] Parent compounds and degradation products were separated and quantified by HPLC. The concentrations were determined from the relative area under the absorbance peaks.

The percentage of analogue degraded over time was calculated vs control to take into consideration the eNPP1-independent degradation of the compounds due to perchloric acid addition at the end of the assay. The percentage of degradation was calculated from the AUC of the NMP peak after subtraction of the control.

Table 2. Enzymatic Stability at 37 °C of Analogues 2−4

		$t_{1/2}$ (h)	
analogue	% hydrolysis of human eNPP1	human blood serum	alkaline phosphatase
ADP	25	2	4
2-MeS-ADP	16	23	4.5
analogue **2**, A isomer	5	3.5	4.2
analogue **3**, A isomer	4	>24	6
analogue **4**, A isomer	0	14	*a*
analogue **4**, B isomer	5	14	*a*

[a]Not hydrolyzed.

Over a 20 min period, ADP was 25% degraded into AMP and Pi, whereas 2-MeS-ADP was only 16% degraded (Table 2). Replacing the Pα oxygen atom with a borane group increased the analogue's stability. Under the same conditions, the A isomers of ADP(α-B) (analogue **2**) and 2-MeS-ADP(α-B) (analogue **3**) were only 5% and 4% degraded, respectively (Table 2). The A and B isomers of 2-MeS-Ap_3(α-B)-A-2-MeS (analogue **4**) were 0% and 5% degraded, respectively (Table 2).

Resistance of Analogues 2−4 to Hydrolysis in Human Blood Serum. Nucleotides and their analogues undergo enzymatic degradation in physiological systems.[38] Blood serum contains nucleotide-hydrolyzing enzymes and, therefore, provides a good model system for assessing the metabolic stability of extracellular nucleotides.

The hydrolysis rates of analogues **2**−**4** in human blood serum prepared from whole blood of healthy volunteers were determined as follows: 40 mM analogue in deionized water, human blood serum (180 μL), and RPMI-1640 medium (540 μL) were incubated at 37 °C for 24 h.[39] Samples were taken every 1 h, and serum enzymes were inactivated by heating at 80 °C for 30 min. As a control, analogues were incubated in the

dx.doi.org/10.1021/jm3006355 | J. Med. Chem. 2012, 55, 7623−7635

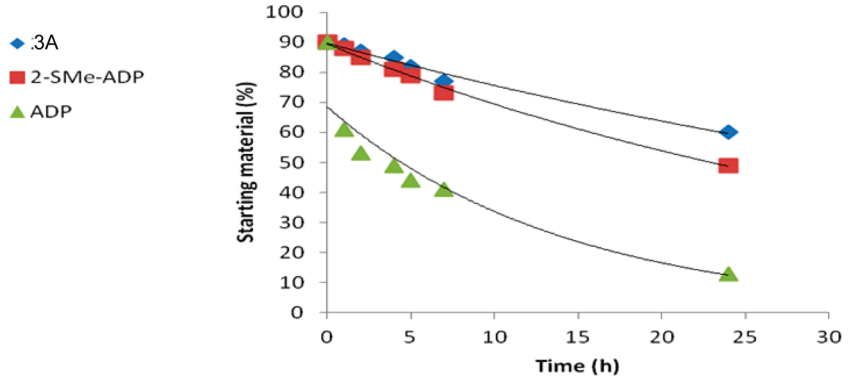

Figure 5. Hydrolysis of ADP, 2-MeS-ADP, and analogue **3A** in human blood serum.

absence of blood serum, to determine the extent of heat-dependent degradation. $T_{1/2}$ values for degradation were determined by measuring the change in the integration of the HPLC peak for each analogue over time. ADP was hydrolyzed with a half-life of 2 h (Figure 5). ADP(α-B), the **2A** isomer, was hydrolyzed with a similar half-life of 3.5 h (Table 2). The half-life of 2-MeS-ADP was found to be 23 h. The **3A** isomer, 2-MeS-ADP(α-B), was highly stable under these conditions with only 40% degraded over 24 h and a half-life similar to 2-MeS-ADP (Figure 5 and Table 2). These results indicate that the borane moiety confers enzymatic stability in human serum for analogue **3A** and the 2-MeS substitution is the main stabilizing factor.

Both A and B isomers of 2-MeS-Ap$_3$(α-B)-A-2-MeS (analogue **4**) exhibited half-lives in human serum of 14 h (Table 2), indicating a 7-fold enhancement compared with the half-life of ADP.

Stability of Analogue 3 at Acidic pH. To explore the suitability of 2-MeS-ADP(α-B) as a drug candidate for oral administration, we evaluated its chemical stability at pH 1.4 at 37 °C, which mimics the acidity of gastric juice. The chemical stability was evaluated for a diastereoisomeric mixture of 2-MeS-ADP(α-B) trisodium salt in KCl/HCl buffer at pH 1.4 and was monitored by HPLC over 12 h. The hydrolysis rate was determined by measuring the change in the integration of the respective HPLC peaks with time to fit a pseudo-first-order reaction model. The hydrolysis rate constant for analogue **3A**/**B** was found to be 2×10^{-5} s^{-1} ($t_{1/2}$ = 7.3 h) (Figure 6).

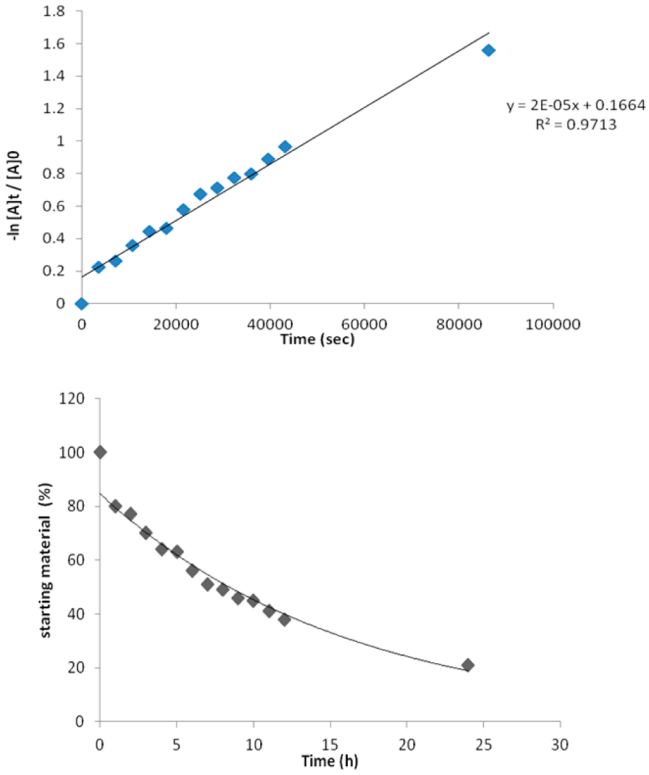

Figure 6. Hydrolysis of analogue **3A** at pH 1.4, 37 °C.

Analogue 3A Decreases Blood Glucose Levels in Both Naïve and Diabetic Animals. Since the A isomer of 2-MeS-ADP(α-B) was found to be a potent and enzymatically stable P2Y$_1$R agonist, *in vivo* studies were performed to test the potential of analogue **3A** administration as a treatment for type II diabetes. Initially, analogue **3A** was evaluated for *in vivo* efficacy in the regulation of glucose homeostasis in rats and mice using an oral glucose tolerance test (OGTT). Rats were studied only in the context of a cross-species proof of principle.

Blood glucose levels of overnight-fasted rats and mice rose quickly after oral administration of a glucose challenge. However, this increase in blood glucose levels was significantly reduced when rats were administered analogue **3A** (30 mg/kg body weight, iv) or glibenclamide (1 mg/kg body weight), a sulfonylurea well-known as an insulin secretagogue. Glibenclamide is administered per os because it is necessary to allocate time for GI absorption and this is the acceptable means of administration in the clinic. Compared with saline administration, analogue **3A** reduced the glucose load within 45 min from 155 to ca. 87 mg/dL, whereas glibenclamide reduced glucose levels to ca. 63 mg/dL, lower than the basal level (Figure 7A). The effect of analogue **3A** on blood glucose levels was also tested at doses of 10 and 30 mg/kg body weight in mice with the higher dose being more effective at reducing the glucose load (Figure 7B). In contrast, analogue **3B** is ineffective when administered at 30 mg/kg body weight (Figure 7C). Moreover, a mixture of analogues **3A** and **3B**, 30 mg/kg total, was less effective than analogue **3A** alone (Figure 7C), suggesting that the diastereoisomers are not equipotent *in vivo* and that separation of the diastereoisomers before administration is preferable.

Being active in naïve animals, analogue **3A** was also tested in two diabetic mouse models. The first model used is chemically induced diabetes, achieved by administration of streptozotocin (STZ), a naturally occurring chemical that is toxic to insulin-producing beta cells in the pancreas of mammals.[40] Mice were given 100 mg/mL STZ intraperitoneally (IP) for 14 days to

dx.doi.org/10.1021/jm3006355 | J. Med. Chem. 2012, 55, 7623−7635

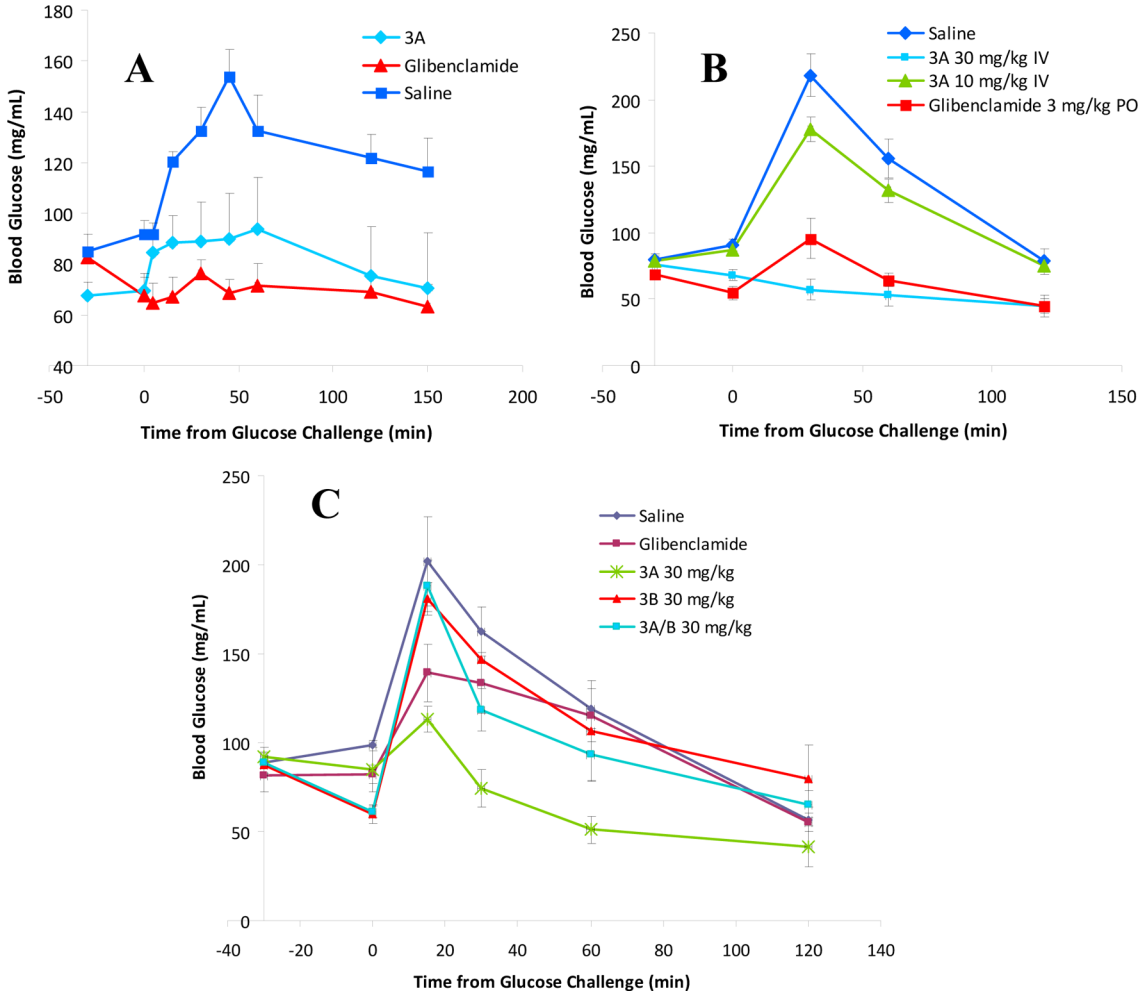

Figure 7. Glucose tolerance tests in naïve mice (n = 5) treated with saline, analogue **3A**, or glibenclamide. Fasting rats (A) and mice (B, C) were treated iv with the indicated compounds at 2.5 mg/kg (A), 10 mg/kg (B) or 30 mg/kg body weight (B, C) 10 min after glucose challenge. Glibenclamide was given orally as a positive control in (A) at 2.5 mg/kg body weight or (B) at 3 mg/kg body weight, 30 min before glucose challenge. Error bars are ± standard deviation.

induce a hyperglycemic response to a glucose challenge. The second diabetic mouse model used is a genetically diabetic mouse (db^+/db^-)[41] that displays elevated basal glucose levels. Analogue **3A** administered at 30 mg/kg was found to lower blood glucose levels to normal values in both models (Figures 8 and 9). The db^+/db^+ (homozygous) mice were not tested with analogue **3A**, because preliminary studies indicate that they are not responsive to sulfonylureas (data not shown).

Analogue 3A Inhibits ADP-Induced Platelet Aggregation. Analogue **3A** was found to be a potent $P2Y_1R$ agonist. Besides lowering blood glucose levels, $P2Y_1R$ agonists have been suggested to initiate platelet aggregation resulting in cardiovascular complications.[42] Thus, the effect of analogue **3A** on platelet aggregation was tested both *in vitro* (using human blood) and *in vivo* (using mice). Exposure of platelet-rich plasma (PRP) to analogue **3A** does not cause platelet aggregation (data not shown), whereas ADP, the endogenous ligand of the $P2Y_1R$, (and the $P2Y_{12}R$) induces platelet aggregation (Figure 10) at low micromolar concentrations.[41] However, analogue **3A** at 0.3−10 μM reduced ADP-induced platelet aggregation in human plasma by 3- and 8-fold, respectively (Figure 10).

The anti-platelet aggregation activity of analogue **3A** is also effective *in vivo*. Normal mice were injected iv with analogue **3A** prior to a tail-cut that produces bleeding, and bleeding time was measured. At a dose of 30 mg/kg body weight, analogue **3A** prolonged tail bleeding time ~1.5-fold, compared with an active metabolite of clopidogrel (R-361015, Daiichi Sankyo; an anti-platelet aggregation agent and antagonist of the $P2Y_{12}R$[44]) (Figure 11). Similar to the dose of analogue **3A** that inhibits platelet aggregation, a dose of 30 mg/kg body weight of analogue **3A** also is effective at lowering blood glucose levels (Figure 7), an important correlation, since diabetic patients frequently suffer from platelet hypersensitivity and cardiovascular disease. The anti-platelet aggregation activity of analogue **3A** *in vivo* is also exhibited upon oral administration. An oral dose of 30 mg/kg body weight of analogue **3A** administered 30 min before tail-cut increased both bleeding time and blood volume in rats, similar to aspirin (Figure 12). Since analogue **3A** is a potent and selective $P2Y_1R$ agonist and the anti-platelet aggregation activity of nucleotide analogues is often attributed to antagonism of the $P2Y_{12}R$,[44] it seems likely that the anti-platelet aggregation effect of analogue **3A** is due to inhibition of $P2Y_{12}R$ activity. Indeed, we found that analogue **3A** displayed partial agonist activity at the $P2Y_{12}R$ relative to the endogenous agonist ADP (Figure 13), thus acting as a $P2Y_{12}R$ antagonist in the presence of ADP.

dx.doi.org/10.1021/jm3006355 | J. Med. Chem. 2012, 55, 7623−7635

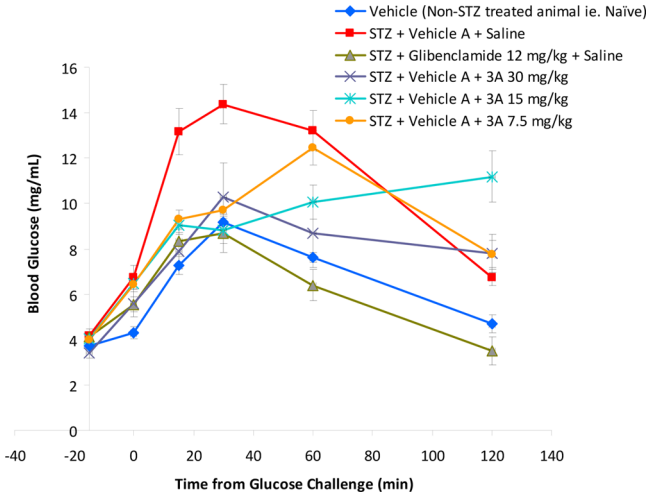

Figure 8. Glucose tolerance tests in the STZ diabetic mouse model. Diabetic (STZ) and normal (blue) mice (n = 5) were administered an OGTT, as described in Figure 7. Three doses of analogue **3A**, 30 (purple), 15 (light blue), and 7.5 (orange) mg/kg body weight, were administered intravenously (iv) and glibenclamide (12 mg/kg body weight, green) was given PO. Saline administration to diabetic mice (red) was used as a control. Error bars are ± standard deviation.

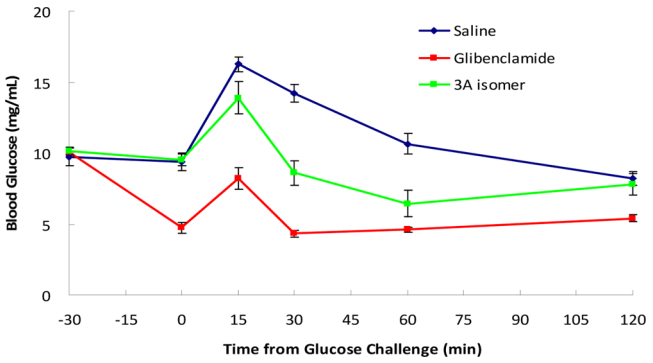

Figure 9. Glucose tolerance tests in the db^+/db^- diabetic mouse model. The db^+/db^- mice were selected for elevated glucose levels. Analogue **3A** (iv, 30 mg/kg body weight, green) and glibenclamide (PO, 20 mg/kg body weight, red) were administered with an OGTT (n = 5), as described in Figure 7. Error bars are ± standard deviation.

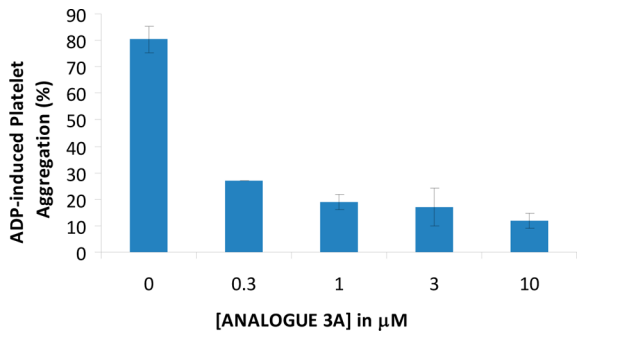

Figure 10. Analogue **3A** inhibits ADP-induced platelet aggregation in human plasma. Analogue **3A** was tested for inhibition of ADP (10 μM) induced platelet aggregation in PRP obtained from one subject in duplicate samples.

DISCUSSION

Sulfonylurea-based insulin secretagogues used for the treatment of type 2 diabetes suffer from various limitations, especially the risk of hypoglycemia. These limitations justify a search for novel insulin secretagogues acting via mechanisms other than the ATP-sensitive K^+ channel, which is activated by sulfonylureas.

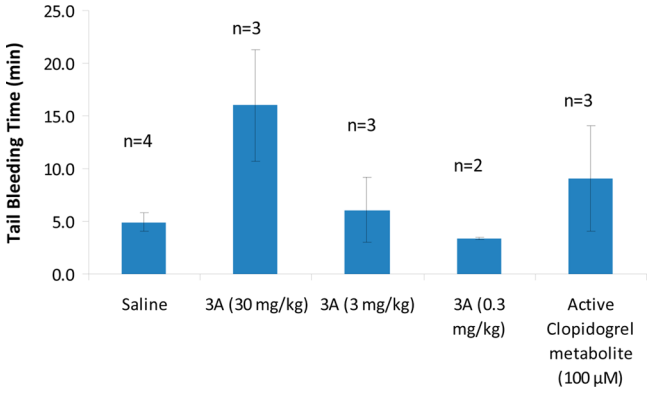

Figure 11. Anti-platelet aggregation activity of analogue **3A** *in vivo*. An increase in mouse tail-bleed time was used as a model for the *in vivo* anti-platelet aggregation activity of analogue **3A** in mg/kg body weight. Mice were treated iv with different doses of analogue **3A** or R-361015, a compound with known anti-platelet aggregation activity, and then the tail was incised and the time to cessation of bleeding was measured. Animal numbers are above bars. Error bars are standard deviation.

Analogue 3A Is a Highly Selective and Potent $P2Y_1R$ Agonist. In the past years, we focused on designing modified nucleotides as drug candidates for the treatment of type 2 diabetes.[15,28] The goal of these modifications to both the adenine (i.e., thioether at C2) and phosphate moieties (i.e., phosphorothioate or boranophosphate) was to improve the potency and selectivity of the nucleotides at the $P2Y_1R$ activation of which mediates insulin secretion and to improve the chemical and metabolic stability of these agonists. A promising drug candidate was 2-methylthio-ATP(α-B), analogue **1A** (Figure 1), which increased insulin secretion by 9-fold above the basal level with an EC_{50} of 28 nM in isolated rat pancreas.[15] Nevertheless, analogue **1A** failed to induce insulin secretion *in vivo*, probably due to its rapid hydrolysis by alkaline phosphatase.[39] Therefore, our approach in the current study was to develop analogues with improved metabolic stability. Instead of ATP(α-B), we synthesized ADP(α-B), analogue **3** (Figure 2). This diphosphate scaffold was predicted to be enzymatically stable because of the proximity of the borane moiety to the cleavage site between Pα and Pβ for alkaline phosphatase, eNPP1, or NTPDase. Furthermore, ADP and ADP analogues modified in the C-2 position are more potent ligands of the $P2Y_1R$ than ATP.[45] In addition, we designed analogue **4** as a potential $P2Y_1R$ agonist based on a diadenosine triphosphate (i.e., Ap_3A) scaffold (Figure 2), since dinucleoside polyphosphates are generally more stable and specific than endogenous nucleotide agonists of P2 receptors.[43] Shaver et al. reported that Ap_3A is a structural analogue of ADP.[46] Both analogues **3** and **4** activated the $P2Y_1R$. At the turkey $P2Y_1R$, analogue **3A** and **3B** isomers exhibited EC_{50} values of 0.038 and 1.1 μM, respectively, and analogue **4A** and **4B** isomers exhibited EC_{50} values of 0.22 and 0.96 μM, respectively (Figure 4), suggesting that these novel analogues have relatively high affinity for the $P2Y_1R$. Analogue **3A**, being the most potent agonist, was selected as the lead candidate for further studies.

$P2Y_1R$ Preferentially Binds the R_p Isomer of Analogue 3 Rather than the S_p Isomer. The diastereoselectivity of the $P2Y_1R$ was demonstrated here very clearly, where the R_p isomer

dx.doi.org/10.1021/jm3006355 | J. Med. Chem. 2012, 55, 7623−7635

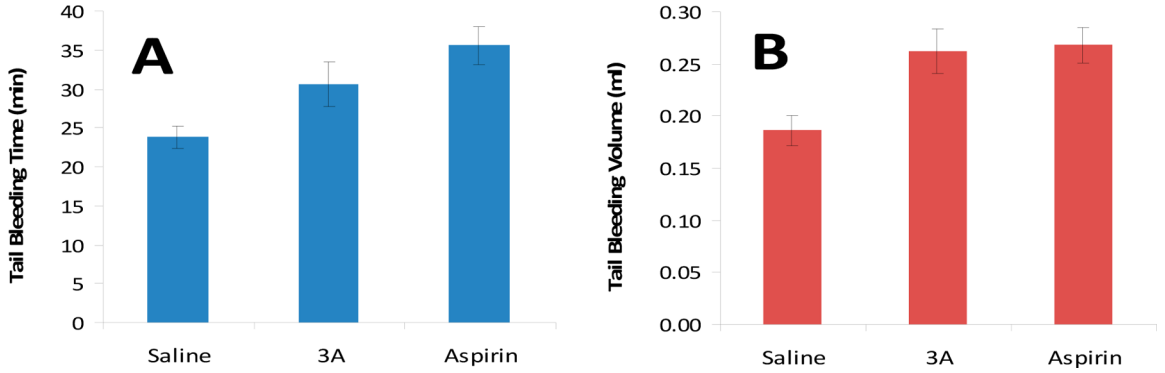

Figure 12. Oral anti-platelet aggregation activity of analogue **3A** *in vivo*. Analogue **3A** (30 mg/kg) or aspirin (10 mg/kg body weight) was administered PO to Lewis rats (n = 5) prior to tail incision, as in Figure 10. Time to cessation of bleeding (A) and total volume of exsanguinated blood (B) was measured. Error bars are ± standard deviation.

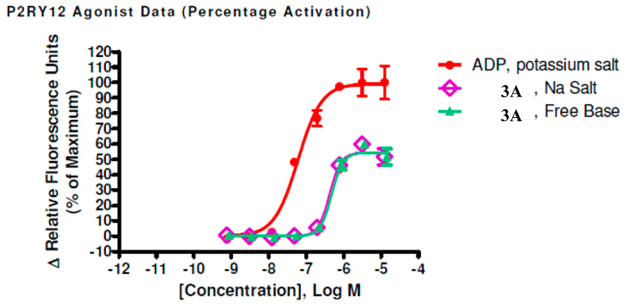

Figure 13. Concentration−response curves for analogue **3A** and ADP were determined by measuring analogue-induced increases in $[Ca^{2+}]_i$ in U-205 cells stably transfected with $hP2Y_{12}R$.

of analogue **3** (**3A**) was 30-fold more active than the S_p isomer of analogue **3** (**3B**). This finding is consistent with our observations in a previous study elucidating the origin of the $P2Y_1Rs$ chiral discrimination.[25] In that study, involving experimental and computational ligand docking data, we found that the Pα pro-*R* oxygen atom of ATP is bound preferentially to the receptor, compared with the pro-*S* oxygen atom.

Thus, in the 2-MeS-ADP-α-B S_p isomer, the Pα *R* oxygen atom is not in the right position to bind the receptor tightly, resulting in a 30-fold higher EC_{50} value than the R_p isomer. Previously, we hypothesized that the $P2Y_1Rs$ chiral discrimination originates from the requirement that the nucleotide agonist interacts with Mg^{2+} ion within the receptor binding site.[25]

Analogue 3A Is an Effective and Safe Drug Candidate for the Treatment of Type 2 Diabetes. STZ-induced diabetes in rodents is commonly used to evaluate efficacy of therapeutic agents. We have carefully calibrated this model to maintain a degree of pancreatic function to demonstrate that treatment with analogue **3A** improves glucose metabolism in STZ-treated mice (Figure 8), presumably via enhanced insulin secretion. Taken together with the reduction in glucose levels following an OGTT in the db^+/db^- mouse (Figure 9), analogue **3A** has the potential to enhance glucose metabolism in diverse diabetes models. Analogue **3A** is also an effective anti-platelet aggregation agent *in vitro* (Figure 10) and can extend bleeding time *in vivo* (Figures 11 and 12). Antithrombotic agents will usually prolong bleeding in animals; however further investigation is required to evaluate the therapeutic modality and efficacy of analogue **3A**. The anti-platelet aggregation activity of analogue **3A** may be attributed to potential antagonism of the $P2Y_{12}R$ subtype.[28]

SUMMARY AND CONCLUSIONS

We developed a novel, potent, selective, and stable $P2Y_1R$ agonist based on an adenosine 5′-*O*-(α-borano)diphosphate scaffold (analogue **3**). Analogue **3A** is a highly potent $P2Y_1R$ agonist with an EC_{50} value of 38 nM. Furthermore, analogue **3A** is chemically stable at gastric juice pH = 1.4 (at 37 °C) with a half-life of 7.3 h. In addition, analogue **3A** proved to be resistant to hydrolysis by human eNPP1, alkaline phosphatase, and blood serum. Acute rodent models of diabetes were used to show the efficacy of analogue **3A** in reducing a blood glucose load to basal levels in naïve rats and mice and hyperglycemic mice, in contrast to reduction to subnormal levels with glibenclamide, a common therapeutic agent for type 2 diabetes. Analogue **3A** also has anti-platelet aggregation activity, possibly due to antagonism of $P2Y_{12}R$ activation by its endogenous ligand ADP. Analogue **3A** is highly soluble in aqueous media and is absorbed orally, suggesting that analogue **3A** is an attractive drug candidate for the treatment of type 2 diabetes.

EXPERIMENTAL SECTION

All air- and moisture-sensitive reactions were carried out in flame-dried, argon-flushed, two-neck flasks sealed with rubber septa, and the reagents were introduced with a syringe. Progress of reactions was monitored by TLC on precoated Merck silica gel plates (60F-254). Column chromatography was performed with Merck silica gel 60 (230−400 mesh). Visualization of reactants and products was accomplished with UV light. Compounds were characterized by nuclear magnetic resonance spectroscopy using Bruker DPX-300 or AC-200 spectrometers. ^1H NMR spectra were measured at 200 or 300 MHz. Nucleotides were characterized also by ^{31}P NMR in D_2O, using 85% H_3PO_4 as an external reference on a Bruker AC-200 spectrometer. Mass spectra were recorded on an AutoSpec-E FISION VG mass spectrometer using ESI (electron spray ionization) on a Q-TOF microinstrument (Waters, UK). Primary purification of the nucleotides was achieved on an LC (Isco UA-6) system using a column of Sephadex DEAE-A25 swollen in 1 M $NaHCO_3$ at 4 °C for 1 day. The resin was washed with deionized water before use. The LC separation was monitored by UV detection at 280 nm. Final purification of the nucleotides and separation of the diastereomeric pairs was achieved on a HPLC (Elite Lachrom, Merck-Hitachi) system using a semipreparative reverse-phase column (Gemini 5 μ C18 110A, 250 × 10 mm^2, 5 μm, Phenomenex, Torrance, USA). The purity of the nucleotides was evaluated by analytical reverse-phase column chromatography (Gemini 5 μ C18 110A, 150 × 4.60 mm^2, 5 μm, Phenomenex, Torrance, USA) with two solvent systems: solvent

dx.doi.org/10.1021/jm3006355 | J. Med. Chem. 2012, 55, 7623−7635

system I (A) CH_3CN/(B) 100 mM triethylammonium acetate (TEAA), pH 7, and solvent system II (A) 0.01 M KH_2PO_4, pH 4.5/(B) MeOH. For analytical purposes, a Gemini 5 μ C18 110A, 150 × 4.60 mm^2, 5 μm column was used. Conditions for LC and HPLC separations are described below. pH measurements were performed with an Orion microcombination pH electrode and a Hanna Instruments pH meter.

All commercial reagents were used without further purification unless otherwise noted. 2-Methylthioadenosine was synthesized from 2-thioadenosine, as described.[47] 2-Thioadenosine was obtained from adenosine in three steps, according to a previously reported procedure.[48] Analogue **2** was synthesized according to the literature.[49] For preparation of human blood serum, whole blood taken from a healthy volunteer was obtained from a blood bank (Tel-Hashomer Hospital, Israel). Blood was stored for 12 h at 4 °C and centrifuged in plastic tubes at 1500*g* for 15 min at RT. The serum was separated and stored at −80 °C.

2-Methylthioadenosine 5′-*O*-(α-Borano)diphosphate (Analogue 3). 2-Methylthio-(2′,3′-*O*-methoxymethylidene) adenosine (253 mg, 0.25 mmol) was dissolved in DMF (1.5 mL)/pyridine (1.25 mmol, 5 equiv). A freshly prepared solution of salicylphosphochloridite (0.275 mmol, 1.1 equiv) in freshly distilled dioxane was then transferred to the flask. After stirring for 10 min, a freshly prepared 1 M solution of bis(tri-*n*-butylammonium) pyrophosphate (0.375 mmol, 1.5 equiv) in DMF and tri-*n*-butylamine (1 mmol, 4 equiv) were simultaneously added. Precipitation occurred immediately after the addition of the reagents, but the precipitate disappeared with further stirring. A 2 M solution of BH_3/Me_2S in THF (2 mmol, 8 equiv) was added, and the mixture was stirred for 15 min. Ethylenediamine (1.25 mmol, 5 equiv) was then added. A white precipitate was immediately formed. After stirring for 60 min, 1 mL of deionized water was added, and the white precipitate gradually dissolved. After 10 min, the reaction mixture was evaporated and then diluted with deionized water and washed twice with ethyl ether. The aqueous layer was freeze-dried, and the semisolid obtained was chromatographed on an activated Sephadex DEAE-A25 column. The resin was washed with deionized water and loaded with the crude reaction residue dissolved in a minimal volume of water. The separation was monitored by UV at 280 nm. A buffer gradient of 400 mL of water to 400 mL of 0.4 M NH_4HCO_3 was used. The relevant fraction was collected and freeze-dried three times until a constant weight was obtained to yield the protected analogue **11** as a white solid. The methoxymethylidene protecting group was removed by acidic hydrolysis (10% HCl solution was added until pH 2.3 was obtained). After 3 h at room temperature, the pH was rapidly raised to 9 by the addition of NH_4OH (pH 11), and the solution was kept at room temperature for 40 min. Analogue **3** was obtained according to the above procedure at 45% yield (274 mg). Final purification and separation of diastereoisomers of analogue **3** were achieved on a semipreparative HPLC column with isocratic elution (B/A, 88:12) with flow rate of 5 mL/min. Fractions containing the same isomer (similar retention time) were freeze-dried. The triethylammonium counterions were exchanged for Na^+ by passing the pure diastereoisomers through a Sephadex-CM C-25 column.

Characterization of 2-Methylthioadenosine 5′-*O*-(α-Borano)diphosphate, A Isomer (Analogue 3A). R_t 14 min. ^{1}H NMR (200 MHz): δ 8.45 (s, H-8, 1H), 5.99 (d, *J* = 5.3 Hz, H-1′, 1H), 4.47 (dd, *J* = 3.8, 4.9 Hz, H-3′, 1H), 4.24 (m, H-4′, 1H), 4.12 (m, H-5′, 2H), 2.59 (S, S−C$\underline{H}_3$, 3H), 0.47 (m, BH_3, 3H) ppm. ^{31}P NMR (200 MHz): δ −83 (m, Pα-BH_3), −6.5 (d, Pβ) ppm. HR MALDI (negative): calculated for $C_{11}H_{19}BN_5O_9P_2S$ 470.134, found 470.139. Purity data obtained on an analytical column: retention time 3.53 min (97% purity) using solvent system I B/A 88:12 with a flow rate of 1 mL/min; retention time 2.15 min (97.5% purity) using solvent system II A/B 5:95 with a flow rate of 1 mL/min.

Characterization of 2-Methylthioadenosine 5′-*O*-(α-Borano)diphosphate, B Isomer (Analogue 3B). R_t 16 min. ^{1}H NMR (200 MHz): δ 8.42 (s, H-8, 1H), 5.99 (d, *J* = 5.6 Hz, H-1′, 1H), 4.39 (dd, *J* = 5, 5.6 Hz, H-3′, 1H), 4.25 (m, H-4′, 1H), 4.12 (m, H-5′, 2H), 2.59 (2S, S−C$\underline{H}_3$, 3H), 0.47 (m, BH_3, 3H) ppm. ^{31}P NMR (200 MHz): δ −84.1 (m, Pα-BH_3), −6.8 (d, Pβ) ppm. Purity data obtained on an analytical column: retention time 4.73 min (97% purity) using solvent system I with a flow rate of 1 mL/min; retention time 3.15 min (98% purity) using solvent system II with a flow rate of 1 mL/min.

P^1-Borano P^1,P^3-5′-Di-2-methylthioadenosine 5′-Triphosphate (Analogue 4). 2-MeS-AMP$(Bu_3NH^+)_2$ (79 mg, 0.184 mmol) was dissolved in dry DMF (2 mL), and CDI (163.7 mg, 0.92 mmol) was added. The resulting solution was stirred at room temperature for 3 h. Dry MeOH (80 μL, 0.92 mmol) was added. After 8 min, 2-MeS-ADP(α-B) $(Bu_3NH^+)_2$ (96 mg, 0.184 mmol) in dry DMF (2 mL) and $MgCl_2$ (4 equiv) were added. The resulting solution was stirred at room temperature overnight. The semisolid obtained after evaporation of the solvent was chromatographed on a Sephadex DEAE-A25 column. A buffer gradient of water (700 mL) to 0.5 M NH_4HCO_3 (700 mL) was applied. The relevant fractions were pooled and freeze-dried to yield a white solid. Final purification and separation of diastereoisomers of analogue **4** were achieved on a semipreparative HPLC column with isocratic elution using solvent system I B/A 88:12 with flow rate of 5 mL/min. Fractions containing the same isomer (similar retention time) were freeze-dried. The triethylammonium counterions were exchanged for Na^+ by passing the pure diastereoisomers through a Sephadex-CM C-25 column.

P^1-Borano P^1,P^3-5′-Di-2-methylthioadenosine 5′-Triphosphate, A Isomer (Analogue 4A). R_t 24.91 min. ^{1}H NMR (200 MHz): δ 8.45 (s, H-8, 1H), 5.99 (d, *J* = 5.3 Hz, H-1′, 1H), 4.47 (dd, *J* = 3.8, 4.9 Hz, H-3′, 1H), 4.24 (m, H-4′, 1H), 4.12 (m, H-5′, 2H), 2.59 (2S, S−C$\underline{H}_3$, 3H), 0.47 (m, BH_3, 3H) ppm. ^{31}P NMR (D_2O, 81 MHz, pH 7): δ 84 (m, Pα, 1P), −11.5 (d, Pα, 1P), −23 (dd, Pβ, 1P) ppm. HR MALDI (negative): calculated for $C_{22}H_{33}BN_{10}O_{18}P_4S_2$ 924.134, found 924.136. Purity data obtained on an analytical column: retention time 4.52 min (96% purity) using solvent system I with a flow rate of 1 mL/min; retention time 3.15 min (97% purity) using solvent system II with a flow rate of 1 mL/min.

P^1-Borano P^1,P^3-5′-Di-2-methylthioadenosine 5′-Triphosphate, B Isomer (Analogue 4B). R_t 29.15 min. ^{1}H NMR (200 MHz): δ 8.42 (s, H-8, 1H), 5.99 (d, *J* = 5.6 Hz, H-1′, 1H), 4.39 (dd, *J* = 5, 5.6 Hz, H-3′, 1H), 4.25 (m, H-4′, 1H), 4.12 (m, H-5′, 2H), 2.59 (2S, S−C$\underline{H}_3$, 3H), 0.47 (m, BH_3, 3H) ppm. ^{31}P NMR (D_2O, 81 MHz, pH 7): δ 84 (m, Pα, 1P), −11 (d, Pα, 1P), −22.5 (dd, Pβ, 1P) ppm. Purity data obtained on an analytical column: retention time 5.62 min (96% purity) using solvent system I B/A 88:12 with a flow rate of 1 mL/min; retention time 4.25 min (96.5% purity) using solvent system II A/B 5:95 with a flow rate of 1 mL/min.

Intracellular Calcium Measurements. Human 1321N1 astrocytoma cells stably expressing the turkey $P2Y_1$ receptor were grown in Dulbecco's modified Eagle's medium containing 5% (v/v) fetal bovine serum, 100 units/mL penicillin, 100 μg/mL streptomycin, and 500 μg/mL Geneticin (G-418; Life Technologies, Inc.). Changes in the intracellular free calcium concentration, $[Ca^{2+}]_i$, were detected by dual-excitation spectrofluorometric analysis of cell suspensions loaded with fura-2, as described previously.[50] Cells were treated with the indicated nucleotide or analogue at 37 °C in 10 mM Hepes-buffered saline (pH 7.4) containing 1 mM $CaCl_2$ and 1 mM $MgCl_2$, and the maximal increase in $[Ca^{2+}]_i$ was determined at various nucleotide or analogue concentrations to calculate the EC_{50}. Concentration−response data were analyzed with the Prism curve fitting program (GraphPAD software, San Diego, CA). Three experiments were conducted on separate days.

Evaluation of the Stability of Analogues 2−4 with Human eNPP1. Human eNPP1 activity was measured at 37 °C in 1 mL of the following incubation medium: (in mM) 1 $CaCl_2$, 200 NaCl, 10 KCl, and 100 Tris, pH 8.5 (Sigma-Aldrich). Then, 0.1 mL of human eNPP1 enzyme preparation[37] (11.2 mg/mL, 6 μL) was added to the reaction mixture, and the mixture was preincubated for 3 min at 37 °C. The reaction was initiated by addition of 0.5 mL of 0.2 mM substrate. The reaction was stopped after 20 min by transferring a 0.3 mL aliquot of the reaction mixture to 0.375 mL of ice-cold 1 M perchloric acid. The samples were centrifuged for 5 min at 10000*g*. Supernatants were neutralized with 1 M KOH at 4 °C and centrifuged for 5 min at 10000*g*. An aliquot of the supernatant (0.2 mL) was analyzed by HPLC to monitor the increase in NMP levels. The percentage of

dx.doi.org/10.1021/jm3006355 | J. Med. Chem. 2012, 55, 7623−7635

substrate hydrolyzed in 20 min corresponds to the average of results from two experiments performed in triplicate.

Evaluation of the Resistance of Analogues 2−4 to Hydrolysis by Alkaline Phosphatase. Alkaline phosphatase (AP) activity was determined by the release of *p*-nitrophenol from *p*-nitrophenyl phosphate measured by a UV−vis spectrophotometer at 405 nm.[51] Relative hydrolysis and resistance to hydrolysis by AP were determined for substrates at 37 °C. A solution of 0.2 mg of analogue in 77.5 μL of deionized water, 0.1 M Tris-HCl, and 0.1 M $MgCl_2$ containing calf intestine alkaline phosphatase (Fermentas Inc., Glen Burnie, MD; 10 units/μL, 1.25 μL, 12.5 units) was incubated at 37 °C. The final pH was 9.8. A sample was taken every 1 h for 8 h. The reaction was stopped by incubation of the sample at 80 °C for 15 min. Each sample was applied to an activated Starta X-AW weak anion exchange cartridge, and the resulting eluate was freeze-dried. Each cartridge was washed with H_2O (1 mL) and MeOH/H_2O (1:1, 1 mL), and the sample was eluted with NH_4OH/MeOH/H_2O (2:25:73, 1 mL), and freeze-dried. The resulting residue was analyzed by HPLC on a Gemini analytical column (5 μ C-18 110A; 150 nm × 4.60 nm). The hydrolysis rates of analogues by alkaline phosphatase were determined by measuring the change in the integration of the HPLC peaks for each analogue over time.

Evaluation of the Stability of Analogues 2−4 in Human Blood Serum. For preparation of human blood serum, whole blood taken from a healthy volunteer was obtained from a blood bank (Tel-Hashomer Hospital, Israel). Blood was stored for 12 h at 4 °C and centrifuged in plastic tubes at 1500*g* for 15 min at RT. The serum was separated and stored at −80 °C. The assay mixture containing 40 mM analogue in deionized water (4.5 μL), human blood serum (180 μL), and RPMI-1640 medium (540 μL)[39] was incubated at 37 °C for 0−24 h, and aliquots were withdrawn at 0.5−12 h intervals. Each sample was then heated to 80 °C for 30 min, treated with CM Sephadex-CM C-25 (1−2 mg), stirred for 2 h using a magnetic stirrer, and centrifuged for 6 min (17000*g*), and the aqueous layer was collected and extracted with chloroform (2 × 500 μL). The aqueous layer was freeze-dried and then dissolved in 100 μL of deionized water. Samples were loaded onto an activated Starta X-AW weak anion exchange cartridge, washed with H_2O (1 mL) and MeOH/H_2O (1:1, 1 mL), eluted with NH_4OH/MeOH/H_2O (2:25:73, 1 mL), and freeze-dried. The resulting residue was analyzed by HPLC on a Gemini analytical column (5 μ C-18 110A; 150 nm × 4.60 nm) at a flow rate of 1 mL/min. The hydrolysis rates of analogues in human blood serum were determined by measuring the change in the integration of the HPLC peaks for each analogue over time.

Evaluation of the Chemical Stability at Acidic pH of 2-Methylthioadenosine 5′-*O*-(α-Borano)diphosphate (Analogue 3). 2-Methylthioadenosine 5′-*O*-(α-borano)diphosphate (1.5 mg) was dissolved in 0.2 M HCl/KCl buffer (0.8 mL), and the final pH was adjusted to 1.4 using 0.2 M HCl. The reaction continued at 37 °C for 24 h with samples taken at 1 h intervals. The stability of 2-methylthioadenosine 5′-*O*-(α-borano)diphosphate was evaluated by HPLC to monitor degradation products using a Gemini analytical column (5 μ C-18 110A; 150 nm × 4.60 nm) and the elution system TEAA/acetonitrile (88:12) at a flow rate of 1 mL/min. The hydrolysis rate of analogue **3** was determined by measuring the change in the integration of the respective HPLC peak with time.

***In Vivo* Study.** *Naïve Animals.* Studies were performed by Vetgenerics Ltd. (Rehovot, Israel). Wister Han male rats and outbred mice (CD-1 mice, a trademark of Charles River Laboratory) were supplied by Harlan Laboratories (Israel). Rats and mice were acclimatized for 6 days prior to commencement of the study and inspected daily for health and welfare throughout the study. For rat studies, animals were weighed, and those most uniform in weight were surgically cannulated, as described below. Cannulated rats were examined for approximately 48 h following surgery to ensure recovery.

Surgical Cannulation Procedure. Rats and mice were anesthetized with 2.5% isoflurane and 97.5% dry air inhalation. Anesthetized rats were secured in the supine position and a 2 cm midline neck incision was fashioned to access the jugular vein and carotid artery. The latter experiment attempted to obtain large amounts of blood for more pharmacodynamic/pharmacokinetic data, but it was very traumatic and labor intensive, so we abandoned this approach and focused on less invasive studies afterward. P52 cannula was surgically inserted and fixed in the jugular vein and flushed with 0.3−0.5 mL of 5% (v/v) heparinized saline after cannulation and also immediately after each blood collection.

Oral Glucose Tolerance Test (OGTT). The function of each cannula was checked in the morning of each experiment. Overnight fasting rats and mice were weighed, and peripheral tail vein blood glucose levels were measured with a glucometer (Abbott Glucometer FreeStyle or FreeStyle Lite), and animals with similar weights and blood glucose levels were assigned to the same group. Rats were left untouched in individual cages for approximately 2 h; mice were housed in treatment groups. Glibenclamide (1 mg/kg body weight) was administrated orally by gavage at $t = -30$ min and then a glucose challenge of 2 g/kg body weight in a volume of 3 mL/kg body weight was orally administrated to each animal at $t = 0$ min. Administration of analogue **3A** or saline control to animals (5 per group) was performed at $t = 10$ min. Analogue **3A** or saline was injected intravenously to both rats and mice via an iv catheter in volumes of 1 mL saline/kg body weight. Blood glucose levels were measured immediately following tail-vein puncture by placing a blood droplet on a glucometer stick inserted into the glucometer.

STZ-Induced Diabetic Mice. Studies were performed by Medicilon (Shanghai, China). Male ICR mice were supplied by Shanghai SINO-British SIPPR/BK Lab Animal Ltd. (Shanghai, China). Environmental controls for animal rooms were set to maintain a temperature of 18−25 °C, humidity of 30−70%, and a 12 h light/12 h dark cycle. Mice were acclimatized for at least 3 days and then selected for the study based on overall good health and acclimation to caging.

Mice were housed 5 per cage. After 4−5 days of acclimatization, mice were randomly selected and treated with STZ (100 mg/kg body weight, IP) after 4 h of fasting. These mice were supplied with 10% glucose water overnight to avoid sudden hypoglycemia postinjection. Control mice were given normal saline. Blood glucose levels and body weights of each mouse were measured on days 4 and 8 post-STZ treatment.

On day 10, the basal blood glucose levels and body weights of each mouse were measured after overnight fasting (about 16 h), 30 min before glucose challenge. STZ-treated mice were grouped according to basal glucose levels. Saline-treated mice were used as the control group. Blood glucose levels of each mouse were evaluated again at 15 min before glucose challenge after dosing with vehicle or 12 mg/kg body weight glibenclamide. Then (0 min time point), an oral dose of 1 g/kg body weight of D-glucose was given to each mouse at 10 mL/kg body weight, and the blood glucose level was measured at 15, 30, 60, and 120 min post-glucose challenge. Three doses of analogue **3A**, either 30, 15, or 7.5 mg/kg body weight, were administered iv, 10 min after glucose administration.

Measurement of Blood Glucose Levels. Monitoring glucose levels in mouse blood was achieved using a OneTouch *Ultra* System (including glucose meter and test strips) from LifeScan Inc. (Milpitas, California, USA). Glucose levels were determined directly in a drop of fresh blood, according to MMPI standard operating procedures for measuring glucose levels in mouse blood.

Diabetic db^+/db^- Mice. Studies were performed by ChemPartner (Shanghai, China). Male db^+/db^- mice at 8 weeks of age were randomly assigned into groups according to body weight and blood glucose levels. Mice were fasted overnight and an OGTT was performed at −30, 0, 15, 30, 60, and 120 min, where 0 min is immediately before glucose administration. Glucose solution at 2 g/kg body weight was administrated by oral gavage. Fifteen minutes before glucose administration, glibenclamide (2 mg/mL in cremophor/EtOH/saline 10:10:80%) was administered by gavage at 10 mL/kg body weight or 20 mg/kg body weight. Blood glucose levels were measured as described above.

Platelet Aggregation. Effects of analogues on platelet aggregation were determined as described in ref 52. PRP (platelet-rich plasma) was produced by centrifuging normal human plasma at 4400*g* for 30 s. PRP (225 μL) was incubated for 15 min at 37 °C before inducing

dx.doi.org/10.1021/jm3006355 | *J. Med. Chem.* 2012, 55, 7623−7635

aggregation with ADP (25 μL, 10 μM; DiaAdin, DiaMed, Cressier, Switzerland), and platelet aggregation was determined after 6 min using the PAP-8E platelet aggregation profiler (BioData, Horsham, PA). The positive control was 10 μM prasugrel metabolite.[53]

Tail-Bleed Assay. Balb/c mice or Lewis rats were anesthetized and then analogues (30, 3, 0.3 mg/kg, mice; 30 mg/kg, rats) or saline were administered intravenously or orally. Aspirin (10 mg/kg body weight) was used as a control in rat experiments. Five minutes later, 2 mm was cut from the tip of the tail using a scalpel, and the tail was placed vertically in a test tube filled with saline. The time to first arrest of bleeding (no bleeding for 20 s) was determined. To determine the volume of blood collected, tubes were spun at 600*g* briefly, and the blood volume was determined visually and compared with known calibrated volumes.

AUTHOR INFORMATION

Corresponding Author

*Fax: 972-3-6354907. Tel: 972-3-5318303. E-mail: bilha.fischer@biu.ac.il.

Author Contributions

‖These authors contributed equally.

Notes

The authors declare no competing financial interest.

¶Patent pending.

ABBREVIATIONS USED

ADP, adenosine 5′-diphosphate; ATP, adenosine 5′-triphosphate; AUC, area under the curve; GPCR, G protein-coupled receptor; HRMS, high-resolution mass spectrometry; LC, liquid chromatography; NMP, nucleoside 5′-monophosphate; eNPPs, ecto-nucleotide pyrophosphatases; P2R, P2 receptor

REFERENCES

(1) Adeghate, E., Ed. Special Issue on Diabetes Mellitus and its Complications: From Molecular Biology to Clinical Medicine. In *Archives of Physiology and Biochemistry*; Swets & Zeitlinger B.V.: Lisse, Netherlands, 2001; Vol. *109*, issue 3, p 96 ff.

(2) Stefek, M., Ed. *Advances in Molecular Mechanisms and Pharmacology of Diabetic Complications*; Transworld Research Network: Kerala, India, 2010; p 341 ff.

(3) Hegarty, B. D.; Turner, N.; Cooney, G. J.; Kraegen, E. W. Insulin resistance and fuel homeostasis: The role of AMP-activated protein kinase. *Acta Physiol.* **2009**, *196*, 129−145.

(4) Scheen, A. J.; Castillo, M. J.; Lefebvre, P. J. Combination of oral antidiabetic drugs and insulin in the treatment of non-insulin-dependent diabetes. *Acta Clin. Belg.* **1993**, *48*, 259−268.

(5) U.K. Prospective Diabetes Study (UKPDS) Group. Intensive blood-glucose control with sulphonylureas or insulin compared with conventional treatment and risk of complications in patients with type 2 diabetes (UKPDS 33). *Lancet* **1998**, *352*, 837−853.

(6) Ishida, H. Mechanism of action of antidiabetic sulfonylureas. *Diabetes Front.* **1999**, *10*, 99−104.

(7) Lebovitz, H. *Oral Antidiabetic Agents*; Lea and Febiger: Philadelphia, PA, 1994; pp 508−529.

(8) Green, J. B.; Feinglos, M. N. Are sulfonylureas passe? *Curr. Diabetes Rep.* **2006**, *6*, 373−377.

(9) Selvin, E.; Bolen, S.; Yeh, H.-C.; Wiley, C.; Wilson Lisa, M.; Marinopoulos Spyridon, S.; Feldman, L.; Vassy, J.; Wilson, R.; Bass Eric, B.; Brancati Frederick, L. Cardiovascular outcomes in trials of oral diabetes medications: a systematic review. *Arch. Intern. Med.* **2008**, *168*, 2070−2080.

(10) Loubatieres-Mariani, M. M.; Chapal, J.; Lignon, F.; Valette, G. Structural specificity of nucleotides for insulin secretory action from the isolated perfused rat pancreas. *Eur. J. Pharmacol.* **1979**, *59*, 277−286.

(11) Chapal, J.; Loubatieres-Mariani, M. M. Effects of phosphate-modified adenine nucleotide analogs on insulin secretion from perfused rat pancreas. *Br. J. Pharmacol.* **1981**, *73*, 105−110.

(12) Hillaire-Buys, D.; Bertrand, G.; Chapal, J.; Puech, R.; Ribes, G.; Loubatieres-Mariani, M. M. Stimulation of insulin secretion and improvement of glucose tolerance in rat and dog by the P2y-purinoceptor agonist, adenosine-5′-O-(2-thiodiphosphate). *Br. J. Pharmacol.* **1993**, *109*, 183−187.

(13) Fernandez-Alvarez, J.; Hillaire-Buys, D.; Loubatieres-Mariani, M. M.; Gomis, R.; Petit, P. P2 receptor agonists stimulate insulin release from human pancreatic islets. *Pancreas* **2001**, *22*, 69−71.

(14) Chapal, J.; Hillaire-Buys, D.; Bertrand, G.; Pujalte, D.; Petit, P.; Loubatieres-Mariani, M. M. Comparative effects of adenosine-5′-triphosphate and related analogs on insulin secretion from the rat pancreas. *Fundam. Clin. Pharmacol.* **1997**, *11*, 537−545.

(15) Farret, A.; Filhol, R.; Linck, N.; Manteghetti, M.; Vignon, J.; Gross, R.; Petit, P. P2Y receptor mediated modulation of insulin release by a novel generation of 2-substituted-5′-O-(1-boranotriphosphate)-adenosine analogues. *Pharm. Res.* **2006**, *23*, 2665−2671.

(16) Leon, C.; Freund, M.; Latchoumanin, O.; Farret, A.; Petit, P.; Cazenave, J.-P.; Gachet, C. The P2Y1 receptor is involved in the maintenance of glucose homeostasis and in insulin secretion in mice. *Purinergic Signalling* **2005**, *1*, 145−151.

(17) Nahum, V.; Zuendorf, G.; Levesque, S. A.; Beaudoin, A. R.; Reiser, G.; Fischer, B. Adenosine 5′-O-(1-boranotriphosphate) derivatives as novel P2Y1 receptor agonists. *J. Med. Chem.* **2002**, *45*, 5384−5396.

(18) Eliahu, S. E.; Camden, J.; Lecka, J.; Weisman, G. A.; Sevigny, J.; Gelinas, S.; Fischer, B. Identification of hydrolytically stable and selective $P2Y_1$ receptor agonists. *Eur. J. Med. Chem.* **2009**, *44*, 1525−1536.

(19) Hoyle, C. H. V.; Hilderman, R. H.; Pintor, J. J.; Schluter, H.; King, B. F. Diadenosine polyphosphates as extracellular signal molecules. *Drug Dev. Res.* **2001**, *52*, 260−273.

(20) Fischer, B.; Boyer, J. L.; Hoyle, C. H. V.; Ziganshin, A. U.; Brizzolara, A. L.; Knight, G. E.; Zimmet, J.; Burnstock, G.; Harden, T. K.; Jacobson, K. A. Identification of potent, selective P2Y-purinoceptor agonists: structure-activity relationships for 2-thioether derivatives of adenosine 5′-triphosphate. *J. Med. Chem.* **1993**, *36*, 3937−3946.

(21) Halbfinger, E.; Major, D. T.; Ritzmann, M.; Ubl, J.; Reiser, G.; Boyer, J. L.; Harden, K. T.; Fischer, B. Molecular recognition of modified adenine nucleotides by the $P2Y_1$-receptor. 1. A synthetic, biochemical, and NMR approach. *J. Med. Chem.* **1999**, *42*, 5325−5337.

(22) Li, P.; Sergueeva, Z. A.; Dobrikov, M.; Shaw, B. R. Nucleoside and oligonucleoside boranophosphates: Chemistry and properties. *Chem. Rev.* **2007**, *107*, 4746−4796.

(23) Burgess, K.; Cook, D. Syntheses of nucleoside triphosphates. *Chem. Rev.* **2000**, *100*, 2047−2059.

(24) Griffin, B. E.; Jarman, M.; Reese, C. B.; Sulston, J. E. The synthesis of oligoribonucleotides. II. Methoxymethylidene derivatives of ribonucleosides and 5′-ribonucleotides. *Tetrahedron* **1967**, *23*, 2301−313.

(25) Major, D. T.; Nahum, V.; Wang, Y.; Reiser, G.; Fischer, B. Molecular recognition in purinergic receptors. 2. Diastereoselectivity of the h-P2Y1-receptor. *J. Med. Chem.* **2004**, *47*, 4405−4416.

(26) Li, P.; Shaw, B. R. Convenient synthesis of nucleoside borane diphosphate analogues: Deoxy- and ribonucleoside 5′-Pα-boranodiphosphates. *J. Org. Chem.* **2004**, *69*, 7051−7057.

(27) Krishnan, P.; Fu, Q.; Lam, W.; Liou, J.-Y.; Dutschman, G.; Cheng, Y.-C. Phosphorylation of pyrimidine deoxynucleoside analog diphosphates: Selective phosphorylation of L-nucleoside analog diphosphates by 3-phosphoglycerate kinase. *J. Biol. Chem.* **2002**, *277*, 5453−5459.

(28) Nahum, V.; Fischer, B. Boranophosphate salts as an excellent mimic of phosphate salts: Preparation, characterization, and properties. *Eur. J. Inorg. Chem.* **2004**, 4124−4131.

(29) Srivastava, P. C.; Robins, R. K.; Meyer, R. B., Jr. In *Chemistry of nucleosides and nucleotides*. Townsend, L. B., Ed.; Plenum Press: New York, 1988; Vol. *1*.

(30) Fujii, A.; Patwari, G. N.; Ebata, T.; Mikami, N. Vibrational spectroscopic evidence of unconventional hydrogen bonds. *Int. J. Mass Spectrom.* **2002**, *220*, 289−312.
(31) Zatorski, A.; Goldstein, B. M.; Colby, T. D.; Jones, J. P.; Pankiewicz, K. W. Potent inhibitors of human inosine monophosphate dehydrogenase type II. Fluorine-substituted analogs of thiazole-4-carboxamide adenine dinucleotide. *J. Med. Chem.* **1995**, *38*, 1098−1105.
(32) Parr, C. E.; Sullivan, D. M.; Paradiso, A. M.; Lazarowski, E. R.; Burch, L. H.; Olsen, J. C.; Erb, L.; Weisman, G. A.; Boucher, R. C.; Turner, J. T. Cloning and expression of a human P2U nucleotide receptor, a target for cystic fibrosis pharmacotherapy. *Proc. Natl. Acad. Sci. U.S.A.* **1994**, *91*, 3275−3279.
(33) Schachter, J. B.; Li, Q.; Boyer, J. L.; Nicholas, R. A.; Harden, T. K. Second messenger cascade specificity and pharmacological selectivity of the human P2Y1-purinoceptor. *Br. J. Pharmacol.* **1996**, *118*, 167−173.
(34) Yelovitch, S.; Camden, J.; Weisman, G. A.; Fischer, B. Boranophosphate isoster controls P2Y receptor subtype selectivity and metabolic stability of dinucleoside polyphosphate analogues. *J. Med. Chem.* **2012**, *55*, 437−448.
(35) Moss, D. W.; Walli, A. K. Intermediates in the hydrolysis of ATP by human alkaline phosphatase. *Biochim. Biophys. Acta, Enzymol.* **1969**, *191*, 476−477.
(36) Harada, M.; Udagawa, N.; Fukasawa, K.; Hiraoka, B. Y.; Mogi, M. Inorganic pyrophosphatase activity of purified bovine pulp alkaline phosphatase at physiological pH. *J. Dent. Res.* **1986**, *65*, 125−127.
(37) Belli, S. I.; Goding, J. W. Biochemical characterization of human PC-1, an enzyme possessing alkaline phosphodiesterase I and nucleotide pyrophosphatase activities. *Eur. J. Biochem.* **1994**, *226*, 433−443.
(38) Gendaszewska-Darmach, E.; Maszewska, M.; Zaklos, M.; Koziolkiewicz, M. Degradation of extracellular nucleotides and their analogs in HeLa and HUVEC cell cultures. *Acta Biochim. Pol.* **2003**, *50*, 973−984.
(39) Eliahu, S.; Barr, H. M.; Camden, J.; Weisman, G. A.; Fischer, B. A novel insulin secretagogue based on a dinucleoside polyphosphate scaffold(1). *J. Med. Chem.* **2010**, *53*, 2472−2481.
(40) Lenzen, S. The mechanisms of alloxan- and streptozotocin-induced diabetes. *Diabetologia* **2008**, *51*, 216−226.
(41) Chung, W. K.; Belfi, K.; Chua, M.; Wiley, J.; Mackintosh, R.; Nicolson, M.; Boozer, C. N.; Leibel, R. L. Heterozygosity for Lepob or Leprdb affects body composition and leptin homeostasis in adult mice. *Am. J. Physiol.* **1998**, *274*, R985−R990.
(42) Boarder, M. R., Webb, T. P2Y receptors: structure and function. In *Purinergic and Pyrimidinergic Signalling*; Abbracchio, M. P., Williams, M., Eds.; Handbook of Experimental Pharmacology, Springer Verlag: Heidelberg, 2001; Vol. *151*, Part 1, pp 65−88.
(43) Jin, J.; Daniel, J. L.; Kunapuli, S. P. Molecular basis for ADP-induced platelet activation. *J. Biol. Chem.* **1998**, *273*, 2030−2034.
(44) Cattaneo, M. New P2Y(12) inhibitors. *Circulation* **2010**, *121*, 171−179.
(45) Ferreira, Z. S.; Silva, C. L. M. *Comparative aspects of purinergic receptors in the phylogenetic scale*; Research Signpost: Kerala, India, 2009; pp 73−91.
(46) Shaver, S. R.; Rideout, J. L.; Pendergast, W.; Douglass, J. G.; Brown, E. G.; Boyer, J. L.; Patel, R. I.; Redick, C. C.; Jones, A. C.; Picher, M.; Yerxa, B. R. Structure-activity relationships of dinucleotides: Potent and selective agonists of P2Y receptors. *Purinergic Signalling* **2005**, *1*, 183−191.
(47) Macfarlane, D. E. 2-Methylthioadenosine [^{32}P]diphosphate: Synthesis and use as probe of platelet ADP receptors. *Methods Enzymol.* **1992**, *215*, 137−142.
(48) Kikugawa, K.; Suehiro, H.; Ichino, M. Platelet aggregation inhibitors. 6. 2-Thioadenosine derivatives. *J. Med. Chem.* **1973**, *16*, 1381−1388.
(49) Li, P.; Xu, Z.; Liu, H.; Wennefors, C. K.; Dobrikov, M. I.; Ludwig, J.; Shaw, B. R. Synthesis of a-P-modified nucleoside diphosphates with ethylenediamine. *J. Am. Chem. Soc.* **2005**, *127*, 16782−16783.
(50) Garrad, R. C.; Otero, M. A.; Erb, L.; Theiss, P. M.; Clarke, L. L.; Gonzalez, F. A.; Turner, J. T.; Weisman, G. A. Structural basis of agonist-induced desensitization and sequestration of the P2Y$_2$ nucleotide receptor. Consequences of truncation of the C terminus. *J. Biol. Chem.* **1998**, *273*, 29437−29444.
(51) Brandenberger, H.; Hanson, R. Spectrophotometric determination of acid and alkaline phosphatases. *Helv. Chim. Acta* **1953**, *36*, 900−906.
(52) Cattaneo, M. Light transmission aggregometry and ATP release for the diagnostic assessment of platelet function. *Semin. Thromb. Hemostasis* **2009**, *35*, 158−167.
(53) Jakubowski, J. A.; Winters, K. J.; Naganuma, H.; Wallentin, L. Prasugrel: A novel thienopyridine antiplatelet agent. A review of preclinical and clinical studies and the mechanistic basis for its distinct antiplatelet profile. *Cardiovasc. Drug Rev.* **2007**, *25*, 357−374.